References

[1]Launder, B. E., and Sharma, B. I., "Application of the Energy Dissipation Model of Turbulence in the Calculation of Flow Near a Spinning Disk," *Letters on Heat and Mass Transfer*, Vol. 1, No. 2, 1974, pp. 131–138.

[2]Wilcox, D. C., "Reassessment of the Scale Determining Equation for Advanced Turbulence Models," *AIAA Journal*, Vol. 26, No. 11, 1988, pp. 1299–1310.

[3]Speziale, C. G., "Analytical Methods for the Development of Reynolds Stress Closures in Turbulence," *Annual Review of Fluid Mechanics*, Vol. 23, 1991, pp. 107–157.

[4]Gatski, T. B., and Speziale, C. G., "On Explicit Algebraic Stress Models for Complex Turbulent Flows," *Journal of Fluid Mechanics*, Vol. 254, 1993, pp. 59–78.

[5]Speziale, C. G., Sarkar, S., and Gatski, T. B., "Modelling the Pressure-Strain Correlation of Turbulence: An Invariant Dynamical System Approach," *Journal of Fluid Mechanics*, Vol. 227, 1991, pp. 245–272.

[6]Abid, R., and Speziale, C. G., "Predicting Equilibrium States with Reynolds Stress Closures in Channel flow and Homogeneous Shear Flow," *Physics of Fluids A*, Vol. 5, No. 7, 1993, pp. 1776–1782.

[7]Durbin, P. A., "Near-Wall Turbulence Models without Damping Functions," *Theoretical and Computational Fluid Dynamics*, Vol. 3, No. 1, 1991, pp. 1–13.

[8]Durbin, P. A., "A Reynolds Stress Model for Near-Wall Turbulence," *Journal of Fluid Mechanics*, Vol. 249, 1993, pp. 465–498.

[9]Yang, Z., and Shih, T. H., "New Time Scale Based K–ε Model for Near-Wall Turbulence," *AIAA Journal*, Vol. 31, No. 7, 1993, pp. 1191–1198.

[10]Patel, V. C., Rodi, W., and Scheuerer, G., "Turbulence Models for Near-Wall and Low Reynolds Number Flows: A Review," *AIAA Journal*, Vol. 23, No. 9, 1985, pp. 1308–1319.

[11]Schubauer, G. B., "Turbulent Processes as Observed in Boundary Layer and Pipe," *Journal of Applied Physics*, Vol. 25, No. 2, 1954, pp. 188–196.

[12]Wieghardt, K., and Tillmann, W., "On the Turbulent Friction Layer for Rising Pressure," NACA TM 1314, Oct. 1951.

[13]Speziale, C. G., Abid, R., and Anderson, E. C., "Critical Evaluation of Two-Equation Models for Near-Wall Turbulence," *AIAA Journal*, Vol. 30, No. 2, 1992, pp. 324–331.

Hypersonic Shockwave/Turbulent Boundary-Layer Interactions on a Porous Surface

Rebecca L. Hanna*
North Carolina State University, Raleigh, North Carolina 27695

Nomenclature

A = van Driest damping factor
C = Darcy parameter
D_v = van Driest damping function
p = pressure
v = velocity normal to streamwise direction
x = distance measured from leading edge of flat plate
x_l = length of flat plate, 36 in.
y = distance measured normal to the surface
δ = boundary-layer thickness
λ = relaxation length
μ_t = eddy viscosity
ρ = density
τ_w = wall shear stress

Subscripts

eq = local
f = end of porous region
p = plenum
r = recovery
s = start of porous region
u = upstream
w = wall

Received Dec. 20, 1994; presented as Paper 95-0005 at the AIAA 33rd Aerospace Sciences Meeting and Exhibit, Reno, NV, Jan. 9–12, 1995; revision received May 24, 1995; accepted for publication May 30, 1995.

*Graduate Research Assistant, Department of Mechanical and Aerospace Engineering. Student Member AIAA.

Introduction

In previous work, Chokani and Squire[1] have shown that under transonic conditions passive control in the form of a porous surface in the region of the shock/boundary-layer interaction weakens the pressure rise through the interaction. The more gradual pressure rise was seen to produce a weaker shock wave and beneficial drag reductions. These authors compared Navier–Stokes calculations and wind-tunnel data and observed the presence of a thin shear layer over the porous surface that was independent of the boundary layer. They suggested that this shear layer altered the effective surface geometry in the interaction region, which provided the mechanism for weakening the shock wave. This observation suggested that shock-induced separation may be delayed or reduced. The presence of the shear layer, however, was also observed in their calculations to increase the skin friction. Since such detailed data were not obtained in the experiment, the numerical investigation was beneficial in order to fully determine if other benefits of passive-control methods outweigh the skin friction penalties.

It has been observed that shock/boundary-layer interactions increase local pressure loads and heat transfer rates in external hypersonic aerodynamic applications; these interactions may, therefore, adversely affect a flight vehicle's lift and drag or may degrade propulsive performance. In this study the passive control of hypersonic shock/boundary-layer interactions is numerically studied. A previously developed Navier–Stokes code is applied, after modifications to the code to account for passive control have been implemented. The predictions of this modified code are then compared with the 28% porosity case experimentally examined by Rallo.[2] The computed solutions are then used to examine details of the interaction region.

Numerical Method

The governing equations are the two-dimensional, unsteady, compressible Navier–Stokes equations. An implicit lower-upper symmetric Gauss–Seidel algorithm is used to obtain steady-state solutions. Complete details of the code used are presented by Morgenstern and Chokani.[3] Some salient features are discussed here.

Wall Boundary Conditions

The upstream upper wall section, including the shock generator, was modeled as an inviscid, impermeable surface. This imposed condition provided both the incident shock and trailing-edge expansion observed in the experiment. The downstream upper wall section was modeled to permit supersonic outflow; this avoided reflection of the recompression shock. The lower surface was a no-slip, impermeable surface; when the passive control was implemented, no-slip, permeable wall conditions were imposed over the region of passive control. On the porous surface, the wall normal velocity was determined by the Darcy pressure-velocity law,

$$v_w = C(p_p - p_w) \tag{1}$$

where the plenum pressure was determined from the requirement that the net mass flux across the porous surface was zero. Two porosity models were examined. In the first case C was held constant at 9.0×10^{-3} m^2 s/kg, which was twice the value used by Chokani and Squire[1] for a 13.6% porous surface and, thus, would closely simulate the 28% porosity. In the second case the parameter C was varied as

$$C = 9.0 \times 10^{-3}\left[0.5 + \sqrt{\sin\left\{\frac{\pi(x - x_s)}{x_f - x_s}\right\}}\right] \tag{2}$$

Assuming a constant value of plenum pressure, the requirement of a net zero mass flux across the porous surface yields this plenum pressure as

$$p_p = \int \rho_w p_w \, dx \Big/ \int \rho_w \, dx \tag{3}$$

Turbulence Model

To model the effects of the fine-scale turbulence, the Baldwin and Lomax eddy viscosity model is used. In the original form this two-layer algebraic model does not account for the upstream (or history) effects. Thus, the relaxation length approach used by Kim and Chokani[4] was also employed:

$$\mu_t = \mu_{t,u} + (\mu_{t,\text{eq}} - \mu_{t,u})[1 - \exp\{-(x - x_u)/(\lambda \delta_u)\}] \tag{4}$$

An initial location x_u and relaxation length λ were required to be provided. A location upstream of the shock/boundary-layer interaction region, where the eddy viscosity reached its equilibrium value, was selected as the initial location. This was in a region where the flow had developed in a nearly zero pressure gradient prior to the interaction. Relaxation lengths of 10 and 30 boundary-layer thicknesses were determined by numerical testing, for the cases without and with passive control, respectively, to give an accurate pressure distribution in the interaction region. The initial locations were $x_u/x_l = 0.607$ and 0.527, respectively.

The original Baldwin and Lomax turbulence model does not account for transpiration effects. Thus, it was necessary to modify the van Driest damping function,

$$D_v = 1 - \exp[-y\sqrt{(|\tau_w/\rho_w|)}/(A\nu_w)] \quad A = 26\exp(-5.9\, v_w^+) \tag{5}$$

This modification effectively accounts for changes in skin friction caused by suction and blowing and provides a more accurate modeling of the fine-scale turbulence effects.

Results and Discussion

The computations employed 171 points in the streamwise direction and 81 points in the streamwise-normal direction. A grid refinement study was conducted in both directions using 171 and 342 points in the streamwise direction and 81 and 162 points in the streamwise-normal direction. The results of the computations using 171 streamwise points and 81 streamwise-normal points showed little difference from the finest grid. All computations were performed on a Cray Y-MP computer. A typical run of 3000 iterations required approximately 250 CPU seconds.

The surface pressure distribution of the computation with the variable porosity model was compared with the experimental results and qualitatively showed the same trends as the experiment. The peak pressure rise in the shock/boundary-layer interaction was well predicted; however, the upstream extent of the interaction was underpredicted by the computation.

A comparison of the predicted pressure distributions of the two porosity models used is shown in Fig. 1. The surface pressure distribution of the inviscid and viscous computations without passive control are also shown for purposes of comparison. The variable porosity model shows a larger increase in the interaction length than the constant porosity model. The constant porosity model also shows an upstream displacement in the location of the shock impingement. Both models, however, show similar reductions in the peak pressure. The velocity vectors shown in Fig. 2 present a more extensive separation than the shock/boundary-layer interaction without passive control. In addition, for the case with porosity, fuller velocity profiles result downstream of the reattachment point. Typical Mach number profiles for both the porous and nonporous cases within the separated flow region are presented in Fig. 3. A significant increase in the height of the subsonic portion of the boundary layer is seen to occur with passive control. This may explain the earlier observation in Fig. 1 of the increased interaction length. The increase in the height of the subsonic region is due to the blowing over the upstream portion of porous region.

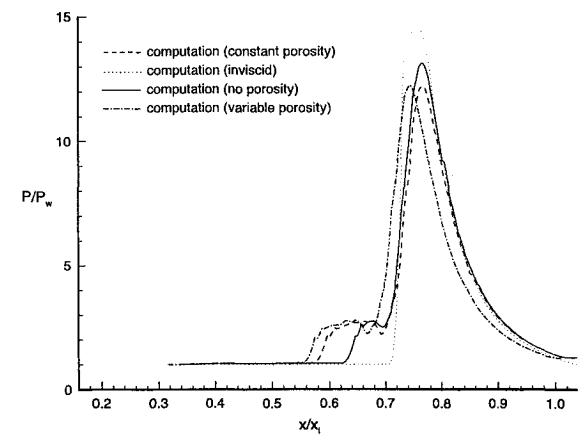

Fig. 1 Comparison of passive control models.

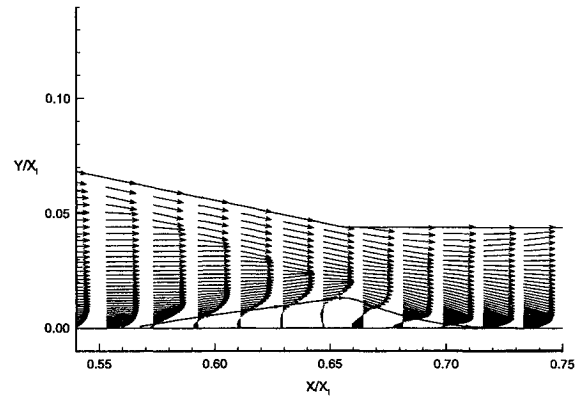

Fig. 2 Velocity vectors; shock/boundary layer interaction region with passive control.

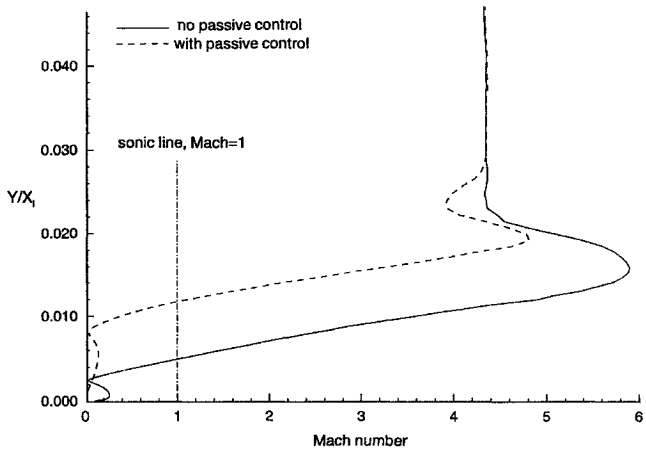

Fig. 3 Comparison of computed Mach number profiles with and without passive control.

Concluding Remarks

The objective of this investigation was to analyze the effects of porosity on the shock wave/boundary-layer interactions of hypersonic flows. Previous studies of these interactions have been inconclusive due the limitations of the available experimental data. In this study a Navier–Stokes code was modified to model the interaction with porosity. The computations show similar trends to the experimental data. With porosity, the interaction length is increased and the peak pressure in the interaction region reduced. The computations also show that the flow separates earlier, indicating that flow separation is not reduced or eliminated with porosity. This is contrary to the observations of transonic interactions. Within the interaction region, an increase in the height of the subsonic portion of the viscous flow is observed. This is attributed to the transpiration of low-subsonic-speed flow introduced as a consequence of the porosity. Downstream of the flow reattachment, fuller profiles result, and

this would suggest a more uniform flow downstream; in practical applications, such as hypersonic flow inlets, this would be desirable. Since the flow separation is not eliminated, however, surface heating penalties may outweigh this benefit. Further studies are required to examine the optimization of the surface porosity. This modified Navier–Stokes code may complement future wind-tunnel testing.

Acknowledgments

The author acknowledges the North Carolina Supercomputing Program for providing computational resources on the Cray Y-MP computer. The author wishes to acknowledge the guidance and patience of Ndaona Chokani, and thanks Algacyr Morgenstern for providing a version of his Navier–Stokes code and discussions concerning its use.

References

[1]Chokani, N., and Squire, L. C., "Transonic Shockwave/Turbulent Boundary Layer Interactions On a Porous Surface," *Aeronautical Journal*, Vol. 97, May 1993, pp. 163–170.

[2]Rallo, R., "An Investigation of Passive Control Methods for Shock-Induced Separation at Hypersonic Speeds," M.S. Thesis, Univ. of Michigan, 1992.

[3]Morgenstern, A., and Chokani, N., "Hypersonic Flow Past Open Cavities," *AIAA Journal*, Vol. 32, No. 12, 1994, pp. 2387–2393.

[4]Kim, I., and Chokani, N., "Navier–Stokes Study of a Supersonic Cavity Flowfield with Passive Control," *Journal of Aircraft*, Vol. 29, No. 2, 1992, pp. 217–223.

Computation of Transonic Flows with Shock-Induced Separation Using Algebraic Turbulence Models

S. K. Chakrabartty* and K. Dhanalakshmi†
National Aerospace Laboratories, Bangalore 560 017, India

Introduction

CONSIDERABLE advancement in the computation of viscous transonic flows using compressible, Reynolds-averaged, Navier–Stokes equations with turbulence models has been achieved recently due to the availability of high-speed computers and the substantial improvement in the efficiency and accuracy of the numerical algorithms. However, for complex flow situations, such as transonic flow past bodies of aerodynamic interest, more effort is necessary to achieve an efficient and reliable solution. The finite volume method is well known for its capability to handle complex geometrical shapes, and it has reached maturity as far as the accuracy of the solution is concerned provided the flow remains laminar and the computational grid is appropriately generated to suit the complexity of the flow and the geometry. However, for turbulent flows, accuracy of the solution depends largely on the turbulence model used to close the system of governing equations. Over the last 20 years the rate of progress in turbulence modeling has been pretty slow compared with that in the development of high-speed computers which, in turn, has led to an increase in the geometrical and fluid mechanical complexity attainable by simulations. The eddy-viscosity-based turbulence models necessarily produce pseudolaminar solutions with the stresses closely linked to the mean-flow gradients; they may be well behaved but they are not usually very accurate away from the flows for which they have been calibrated. Turbulence models based on term-by-term modeling of the Reynolds-stress transport equations produce solutions which may be accurate in some cases but are liable to fail rather badly in other cases; that is, they are ill behaved in a way that eddy-viscosity methods are not.[1] Algebraic turbulence models[2–4] have been extended by others far beyond the domain intended by their originators because of their simplicity in use and the virtue of almost never breaking down computationally.

Finite volume spatial discretization with Runge–Kutta time stepping scheme developed for the Euler equations has been successfully extended by Swanson and Turkel[5] to the viscous flow computation using thin-layer Navier–Stokes equations, and similar procedures are being used by many others.[6,7] These methods follow cell-centered finite volume formulation, where the flow quantities are associated with the center of a cell in the computational mesh and the fluxes across the cell boundaries are calculated using arithmetic means of the values in the adjacent cells. In these schemes the procedure used to compute the pressure on the boundary incorporates the boundary-layer type of approximation, i.e., the zero normal pressure gradient inside the boundary layer. However, in real flows, the normal pressure gradient is not negligible and it may cause confusion in tests of turbulence models.

On the other hand, cell-vertex or nodal point schemes proposed by Ni[8] and Hall[9] for Euler equations have been extended to solve Navier–Stokes equations originally presented by Chakrabartty[10,11] and later used and extended to three dimensions by Radespiel[12] with thin-layer approximation. The main advantages of the vertex-based schemes over cell-centered schemes are 1) the accuracy in the computations of derivatives, particularly for stretched and skewed grids and 2) direct computation of pressure on the wall. A novel vertex-based (nodal point) spatial discretization scheme in the frame work of finite volume method has been proposed by Chakrabartty,[13] which gives second-order accurate first derivatives and at least first-order accurate second derivatives even for stretched and skewed grids. This scheme takes almost the same numerical effort to solve full Reynolds-averaged Navier–Stokes equations as that for thin-layer approximation.

In the present work, the finite volume method based on the nodal point approach introduced earlier in Ref. 13 has been used with algebraic turbulence models proposed by Cebeci and Smith[2,3] and Baldwin and Lomax.[4] Further improvements of these basic models proposed by Radespiel[12] and Goldberg[14] for separated flows have been implemented and studied by computing three typical examples having strong shocks with shock-induced separated bubble. The details regarding the governing equations, boundary conditions, finite volume space discretization, the five-stage Runge–Kutta time stepping and the acceleration techniques are available in Ref. 13.

Turbulence Modeling

Algebraic turbulence modeling introduced by Cebeci and Smith[2,3] and later modified by Baldwin and Lomax[4] for the outer region, where the necessity to compute the displacement thickness for the eddy length scale was replaced by the local vorticity, works well for attached flows. Transonic flows with strong shocks exhibit a small separation bubble at the foot of the shock. Existing turbulence models either do not treat such bubbles or do so in an ad hoc fashion. Goldberg[14] attempted to address this problem in a rigorous manner and proposed a model to treat the separated region. His model is based on the assumption and observation that 1) the stress scale is given by the maximum shear stress in the separated layer, not by the wall stress as proposed by Baldwin and Lomax and 2) the shear layer has qualitatively the same turbulent structure when it is detached as when it is attached and the length scale is the height of the separated region. Radespiel[12] also used a similar idea by replacing the distance from the wall by the distance from the minimum velocity line (see Fig. 1 for nomenclature) and the shear stress at the wall by its maximum value to prevent vanishing eddy viscosity at the separation point. He, however, did not treat the region between the wall and the minimum velocity line. He obtained a pressure distribution with stronger shock downstream of the experimental

Received Aug. 15, 1994; revision received Dec. 9, 1994; accepted for publication Jan. 20, 1995.

*Scientist, Computational and Theoretical Fluid Dynamics Division. Senior Member AIAA.

†Scientist, Computational and Theoretical Fluid Dynamics Division.